SiPM detectors for the ASTRI project in the framework of the Cherenkov Telescope Array

Sergio Billotta*[a], Davide Marano[a], Giovanni Bonanno[a], Massimiliano Belluso[a], Alessandro Grillo[a], Salvatore Garozzo[a], Giuseppe Romeo[a], Maria Cristina Timpanaro[a], Maria Concetta Maccarone[b], Osvaldo Catalano[b], Giovanni La Rosa[b], Giuseppe Sottile[b], Domenico Impiombato[b], Carmelo Gargano[b], Salvatore Giarrusso[b] for the ASTRI Collaboration[c] and the CTA Consortium[d]

[a]INAF, Osservatorio Astrofisico di Catania, Via S. Sofia 78, I-95123 Catania (Italy);
[b]INAF, Istituto di Astrofisica Spaziale e Fisica Cosmica di Palermo, Via U. La Malfa 153, I-90146 Palermo (Italy)
[c]http://www.brera.inaf.it/astri/
[d]http://www.cta-observatory.org/

ABSTRACT

The Cherenkov Telescope Array (CTA) is a worldwide new generation project aimed at realizing an array of a hundred ground based gamma-ray telescopes. ASTRI (*Astrofisica con Specchi a Tecnologia Replicante Italiana*) is the Italian project whose primary target is the development of an end-to-end prototype, named ASTRI SST-2M, of the CTA small size class of telescopes devoted to investigation of the highest energy region, from 1 to 100 TeV. Next target is the implementation of an ASTRI/CTA mini-array based on seven identical telescopes. Silicon Photo-Multipliers (SiPMs) are the semiconductor photosensor devices designated to constitute the camera detection system at the focal plane of the ASTRI telescopes. SiPM photosensors are suitable for the detection of the Cherenkov flashes, since they are very fast and sensitive to the light in the 300-700nm wavelength spectrum. Their drawbacks compared to the traditional photo-multiplier tubes are high dark count rates, after-pulsing and optical cross-talk contributions, and intrinsic gains strongly dependent on temperature. Nonetheless, for a single pixel, the dark count rate is well below the Night Sky Background, the effects of cross-talk and afterpulses are typically lower than 20%, and the gain can be kept stable against temperature variations by means of adequate bias voltage compensation strategies. This work presents and discusses some experimental results from a large set of measurements performed on the SiPM sensors to be used for the ASTRI SST-2M prototype camera and on recently developed detectors demonstrating outstanding performance for the future evolution of the project in the ASTRI/CTA mini-array.

Keywords: ASTRI, CTA, detectors, characterizations, photon detection efficiency, silicon photomultipliers.

1. INTRODUCTION

The upcoming Cherenkov Telescope Array (CTA) is a worldwide project focused on the design, realization and operation of an array of a hundred ground based new generation gamma-ray telescopes covering a wide energy range with a sensitivity in the core energy region (around 1 TeV) of nearly one order of magnitude greater than currently operating telescope arrays. Due to the different characteristics of the Cherenkov light signals within different energy bands, three kinds of telescope configurations will be implemented in order to provide the widest coverage of the energy spectrum: the low energy band (from 20 GeV up to 1 TeV) will be covered by large-size telescopes (LSTs) with 23-m diameter mirrors; the medium energy region (from 200 GeV up to 10 TeV) will be observed by medium-size telescopes (MSTs) with 12-m diameter mirrors; the highest energy band (from few TeV to 100 TeV) will be detected by small-size telescopes (SSTs) with 4-m diameter mirrors [1]. Two arrays will be deployed, one in the Northern and one in the Southern hemisphere, in order to provide all-sky coverage.

ASTRI (*Astrofisica con Specchi a Tecnologia Replicante Italiana*) is a flagship project financed by the Italian Ministry of Education, University and Research (MIUR) and led by the Italian National Institute for Astrophysics (INAF), strictly linked to the development of the CTA. Primary target of the ASTRI project is the development of an end-to-end

* sergio.billotta@oact.inaf.it; phone +39-95-7332205.

High Energy, Optical, and Infrared Detectors for Astronomy VI, edited by Andrew D. Holland, James Beletic, Proc. of SPIE Vol. 9154, 91541R · © 2014 SPIE · CCC code: 0277-786X/14/$18 · doi: 10.1117/12.2055331

prototype of the SST telescopes. The prototype is characterized by innovative technological solutions in terms of mirror structure, focal plane sensors and front-end electronics. The prototype is under construction and will be installed and commissioned by the end of 2014 at the INAF "M.G. Fracastoro" observing station (1735m a.s.l.) located in Serra La Nave, on Mount Etna (Catania, Sicily) [2]. The prototype is expected to be fully operative under field conditions in the early months of 2015.

The ASTRI prototype (henceforth referred to as SST-2M) will be equipped with a wide field dual-mirror (2M) Schwarzschild-Couder (SC) optical system arranged in a compact layout configuration, empowering good angular resolution across the entire field of view (almost 10° in diameter) and reducing the effective focal length and camera dimensions. The optical approach adopted allows the exploitation of a compact, low-cost, light-weight and low-power consumption camera to be placed at the curved focal surface of the telescope [3]-[4].

Silicon Photo-Multipliers (SiPMs) are the semiconductor photosensor devices intended to equip the camera at the focal plane of the ASTRI SST-2M telescope. SiPM detectors operate at a relatively low bias voltage and feature high multiplication ratio, high photon detection efficiency, fast transient response, excellent time resolution and wide spectral response range; therefore, they can be used in photon counting applications and have a strong inherent potential for replacing traditional phototube detectors. Since the last few years, SiPM technology has been developing very quickly; new SiPM detectors with outstanding characteristics have been recently produced by the world leading manufacturers and further performance improvements are foreseen at short terms. Contextually, remarkable research activities have been worldwide undertaken by a rising number of companies and institutions [5]-[17].

SiPMs basically have a physical structure in which combinations of a Geiger-mode Avalanche PhotoDiode (G-APD), also known as Single-Photon Avalanche Diode (SPAD) [5]-[6], and a series quenching resistor create a single pixel microcell; they are connected in parallel and bi-dimensionally arranged to realize the SiPM structure as in Figure 1.

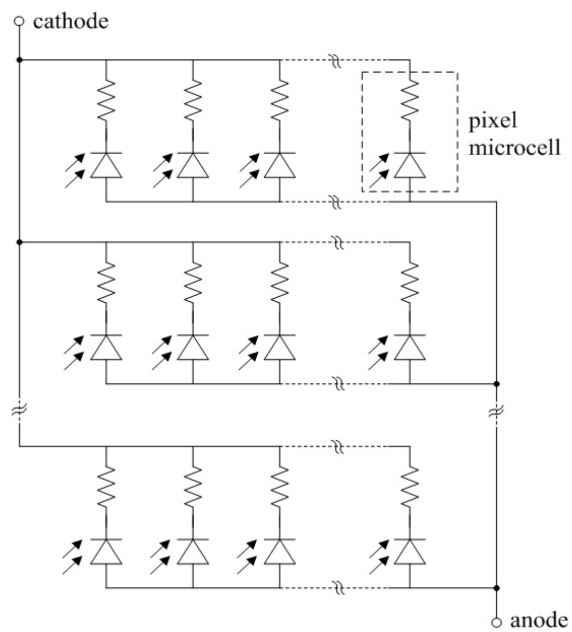

Figure 1. Simplified equivalent circuit of a SiPM detector as a parallel connection of single basic pixel microcells.

Every elementary microcell independently detects an avalanche event and determines whether a photon has entered the pixel. The output signal produced when one or more photons are detected keeps constant regardless of the number of input photons, meaning that each single SPAD micro-pixel only provides information on whether a photon is received. Since a SiPM detector consists of multiple microcells sharing the same cathode and anode terminals, the output current signal is the sum of all single SPAD currents, therefore indicating the total number of fired microcells. The quenching resistance integrated in each single pixel allows the avalanche current to flow through the photodiode but does not allow a self-sustained avalanche, since it limits the asymptotic steady-state value of this current. All basic micro-pixels are connected to a unique readout channel, so that the current pulses overlap with each other generating a single output signal.

SiPM photosensors are suitable for the detection of the Cherenkov flashes, since they are very fast and sensitive to the light in the 350-700 nm wavelength range. Their drawbacks compared to the traditional photo-multiplier tubes, so far used in Cherenkov telescopes, are high dark count rates, spurious after-pulsing, optical cross-talk contributions, and intrinsic gain factors strongly dependent on chip temperature. Nonetheless, the SiPM dark count rate is well below the Night Sky Background (NSB), so that the instrumental background does not degrade the telescope sensitivity; in addition, the effects of cross-talk and afterpulses are typically restrained, and the gain can be kept stable against temperature variations by means of an adequate bias voltage compensation strategy.

The construction, commissioning and first observational campaigns of the ASTRI SST-2M prototype will allow an accurate testing of all telescope components (mechanics, mirrors, camera, front-end electronics) in real observing conditions, in order to confirm the effectiveness of the technological solutions adopted and verify the telescope expected performance. Although the ASTRI SST-2M telescope will mainly act as a technological prototype, it should be able to perform scientific observations as well. The ASTRI collaboration proposed the installation of a small array of 7 SST-2M telescopes at the selected CTA Southern site. This ASTRI/CTA mini-array [18] will constitute the first CTA seed and could be used for technical purposes and scientific studies, mainly in the highest energy region from few tens of TeV. This energy region is still widely unexplored and may lead to new unexpected discoveries.

In the following, some experimental results from a large set of measurements performed on the SiPM sensors to be used for the ASTRI SST-2M telescope camera are presented, in order to characterize the detector performance and confirming its compliance with the telescope focal plane requirements.

2. THE ASTRI SST-2M CAMERA

The ASTRI SST-2M camera [3], [19] has a truncated-cone shape with overall dimensions of about 50cm×50cm×50cm, including mechanics and interfaces with the telescope structure, for a global weight around 50kg. Such detection surface requires a spatial segmentation of a few square millimeters to be compliant with the imaging resolving angular size (0.17°). Furthermore, the light sensor should offer a high photon detection sensitivity in the wavelength range between 300nm and 700nm and a fast temporal response.

In order to match the angular resolution of the optical system, the design of the ASTRI camera has to comply with the general idea of modularity. In other words, particular care has been devoted to the choice of dimensions for the basic detection module. Since the convex-shaped focal surface of the SST-2M camera has a curvature radius of about 1 meter, the curved surface of the camera has to be fit with a certain number of square modules without losing the required focusing capability of the optical system. This specification is physically accomplished by a pixel of about 6.2×6.2mm^2, resulting in a sky-projected angular size of 0.17°.

Since the energy working range of the ASTRI SST-2M telescope is in the order of 10-100TeV, the maximum number of photoelectrons detected in a single pixel, also according to the optics area, is estimated to be 1000, collected in a very short time duration (few nanoseconds).

Among the available SiPM sensors, the Hamamatsu S11828-3344 Multi-Pixel Photon Counter (MPPC) device has been selected for the ASTRI SST-2M prototype. The basic detector unit provided by the manufacturer is a monolithic multi-pixel MPPC consisting of a 4×4 matrix of squared SiPM pixels, each of which has an area of 3×3mm^2 and is made up of 3600 elementary photodiode microcells (SPADs) of 50-μm pitch with a 62% geometrical fill factor. Four SiPM pixels are physically grouped together into a unique logical macro-pixel with an overall physical size of 6.2×6.2mm^2, corresponding to the required 0.17° optical angular resolution. A modular electronic unit (Photon Detection Module, PDM) is realized stacking three different PCBs: an upper board containing 4x4 Hamamatsu MPPCs (for a total of 8x8 macro-pixels) with overall 56×56mm^2 dimensions, an inner board (Front-End Electronics, FEE) hosting two 32-input ASICs and four 14-bit Analog-to-Digital Converters (ADCs) devoted to SiPM readout, and a lower board containing the Field Programmable Gate Array (FPGA) which manages the ASICs slow control, local triggers generation and digital data acquisition.

At the focal plane of the telescope camera 37 structural PDM tiles are combined together, delivering the required full optical field of view. To prevent accidental sunlight exposure of the focal surface detectors, the ASTRI SST-2M camera is equipped with a light-tight two-petal lid mounted onto the backbone structure of the camera. Figure 2 depicts an overview of the camera box, on top of which the 37 PDM modules are visible.

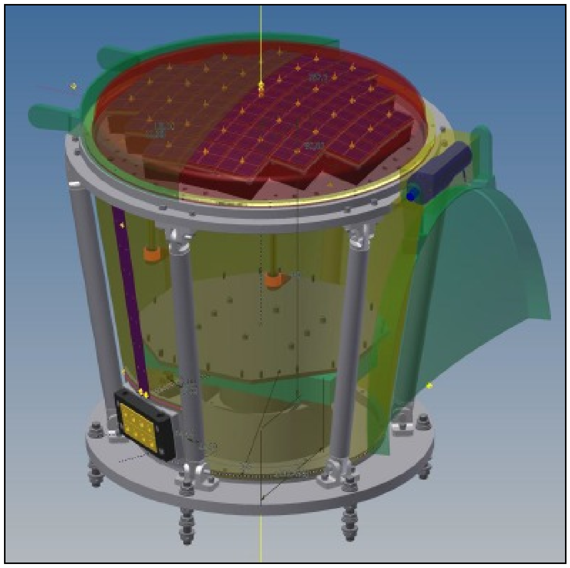

Figure 2. Overall schematic of the ASTRI SST-2M telescope camera, with the 37 structural PDMs at the focal plane.

The main element of the ASTRI SST-2M camera FEE is the Cherenkov Image Telescope Integrated Read Out Chip (CITIROC) [20], produced by Omega. It is a 32-channel fully-analog front-end ASICs specifically designed to directly interface SiPM detectors, working as signal shapers. The SiPM signal is integrated by a CITIROC channel over a given time window, and the CITIROC channel outputs an analog signal whose amplitude represents the value of the integrated input signal.

The main advantage of the ASTRI SST-2M camera design is that all basic PDMs are physically independent of each other, simplifying the maintenance of the camera. Furthermore, in consideration of the rapidly developing progress and innovation of SiPM fabrication technology, the mechanical structure and front-end electronics of the telescope camera are specifically designed such that the detectors of each single PDM can be easily substituted with different SiPM sensors of the same logical pixel dimensions.

3. MEASUREMENT APPARATUS

In the following, the experimental apparatus engaged for the detector characterization is briefly discussed.

3.1 Measurement Set-up

The experimental set-up exploited for the optical characterizations of solid-state detectors is one of the available facilities at the Catania astrophysical Observatory Laboratory for Detectors (COLD) within INAF, Osservatorio Astrofisico di Catania. The basic equipment used for SiPMs characterization is illustrated in Figure 3.

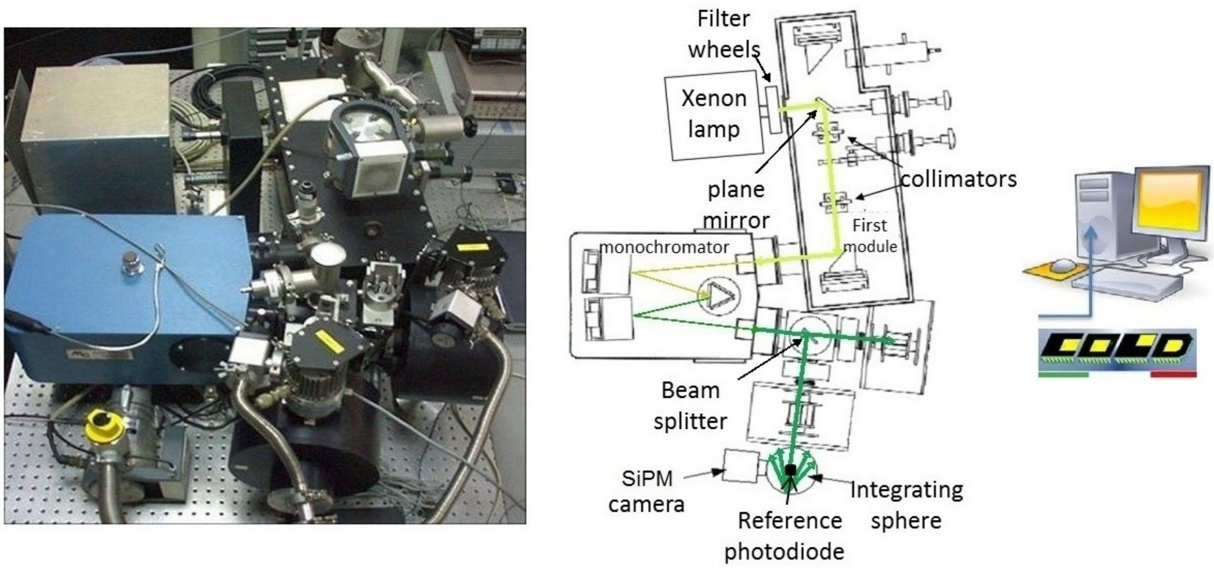

Figure 3. Simplified schematization of the COLD optical apparatus. On the left side: photograph of the characterization equipment. On the right side: scheme of the implemented mechanical and optical parts of the apparatus, where the green line indicates the light path.

A Xenon lamp is used as a radiation source; a wavelength selection system constituted by a set of band-pass filters and mirrors, and a Czerny-Turner monochromator are exploited to achieve the desired wavelength in the 130-1100nm spectral range, with a FWHM smaller than 1nm. A beam splitter is employed to direct the monochromatic radiation through an optical lens towards an integrating sphere, which hosts, in one port, a 1-cm^2 NIST-traced reference photodiode and, in a second port, the SiPM sensor to be characterized. The photon flux intensity coming into the integrating sphere can be regulated by means of neutral density filters or changing the aperture of the entrance or exit slits of the monochromator. Due to the small dimensions of the detectors to be characterized with respect to the optical beam, the integrating sphere is used to spatially integrate the radiant flux. Furthermore, appropriate mechanical structures are realized, in terms of both aperture and distance from the centre of the sphere, to illuminate the SiPM detector and the NIST-traced photodiode with the same radiant flux. The reference photodiode allows to evaluate the number of photons per unit area, and then, after a proper rescaling, the number of photons impinging on the detectors under test.

The electronic system exploited for biasing the SiPM detectors and amplifying its output pulses is the CAEN PSAU (Power Supply and Amplification Unit). It provides the cathode voltage for the SiPM detector in a range of 0-120V with a 16-bit resolution, and features a variable amplification factor up to 50dB. It integrates a feedback circuit to stabilize the operating voltage (and, in turn, the sensor gain) against thermal variations and a leading edge discriminator feeding an internal counter. In addition, the system can provide a digital output with a tunable width from 20ns to 320ns. All parameters can be programmed and monitored via a standard USB interface.

3.2 SiPM Interface Systems

The instrumental set-up developed at the COLD laboratory is aimed at providing future systematic characterization of the MPPC detectors of a complete PDM, constituting the basic structural unit of the camera at the focal plane of the ASTRI SST-2M telescope.

The way the detectors are assembled in a PDM module is illustrated in Figure 4, showing a pictorial schematization of the baseline focal surface arrangement. Each SiPM unit consists of 4 logical channels, so that a complete PDM module is constituted by 64 logical macro-pixels. In total, 37 structural modules are required to convey the information represented by photoelectron pulse signals coming from the focal surface camera detectors. The single macro-pixel constituting the basic logical channel is highlighted in the picture by the yellow square box.

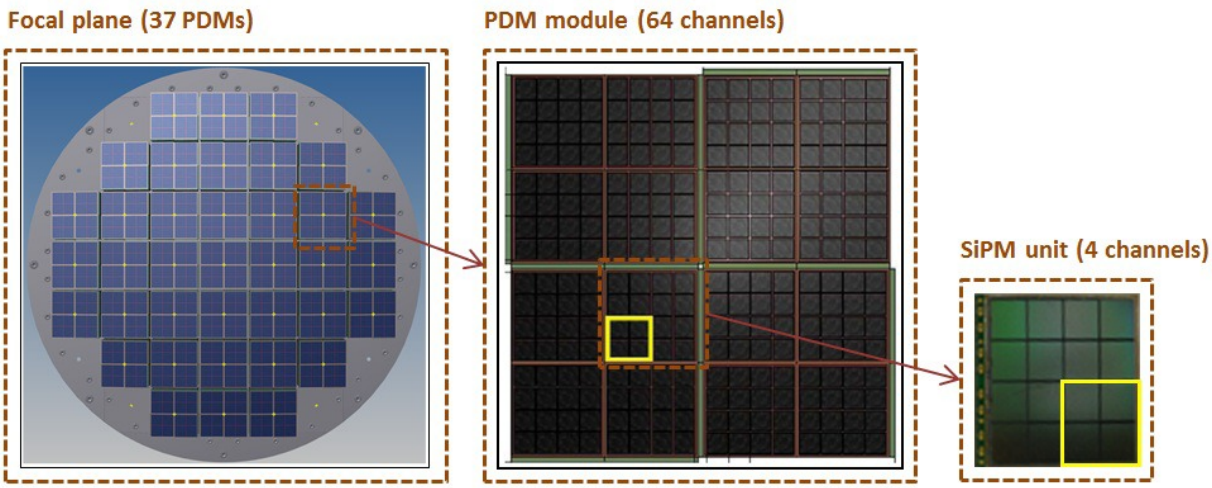

Figure 4. Structural composition of the PDM modules on the ASTRI SST-2M telescope focal plane.

The PCB board realized to interface the MPPC detectors and the FEE is depicted in Figure 5.

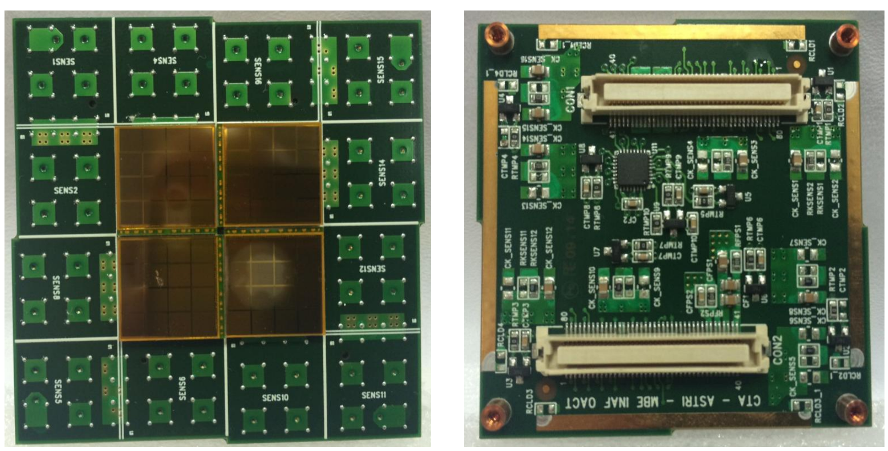

Figure 5. SiPM interface board top layer (on the left side) and bottom layer (on the right side).

On top of the board the 4 anodes of each monolithic MPPC are connected together while a common pin is used for all cathodes. The MPPC detectors are soldered so as to conform with the mechanical structure of the board. The bottom layer of the board hosts two multi-pin connectors interfacing with the FEE, along with 8 R-C filters for the MPPC voltage supply and 9 temperature sensors for gain stabilization, connected to an analog multiplexer.

Tests have been carried out connecting a SiPM interface board to an evaluation board of a previous version of CITIROC, the Extended Analogue SiPM Integrated Read-Out Chip (EASIROC) [21], whose performance are similar to the CITIROC ASIC for the measurements performed.

To allow a versatile interface between the 64 SiPM signals and the 32 input channels of the EASIROC evaluation board, an adapter board, shown in Figure 6, has been realized at the COLD laboratory for testing purposes. Due to the 32 input channels of EASIROC, two multi-pin connectors on the adapter PCB receive the 64 detector output signals from the SiPM interface board, which are routed towards two 32-pin strip connectors located on the rear side of the adapter board.

As a result, one strip connector at a time can couple 32 output signals from each SiPM interface board (half of the available logical pixels) to the EASIROC evaluation board. In this way, each complete SiPM interface board can be characterized by simply rotating the position of the adapter PCB and connecting both strips to the EASIROC board.

Furthermore, a DIP-switch assembled on top of the board allows an individual selection of the outputs of the temperature sensors in the SiPM interface board, managing the analog multiplexer outputs.

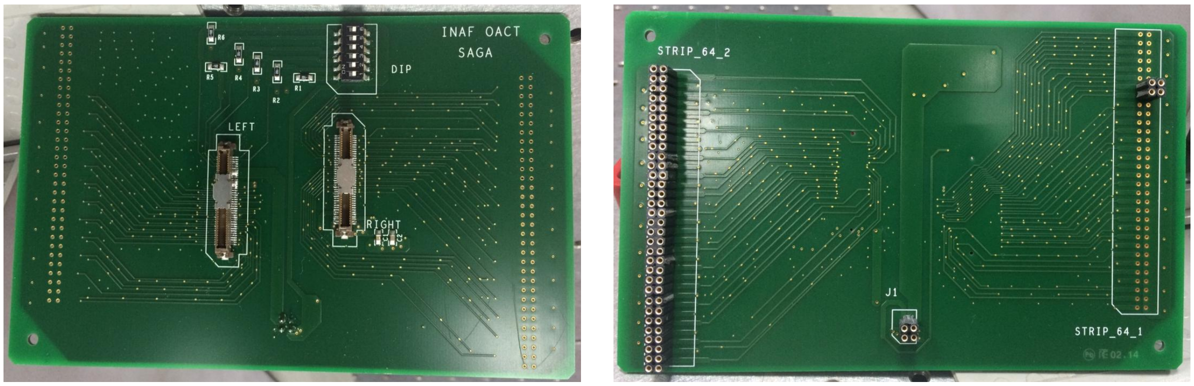

Figure 6. SiPM adapter board top layer (on the left side) and bottom layer (on the right side).

A photograph of the SiPM interface board with the 16 monolithic MPPC devices connected to the adapter board is shown in Figure 7.

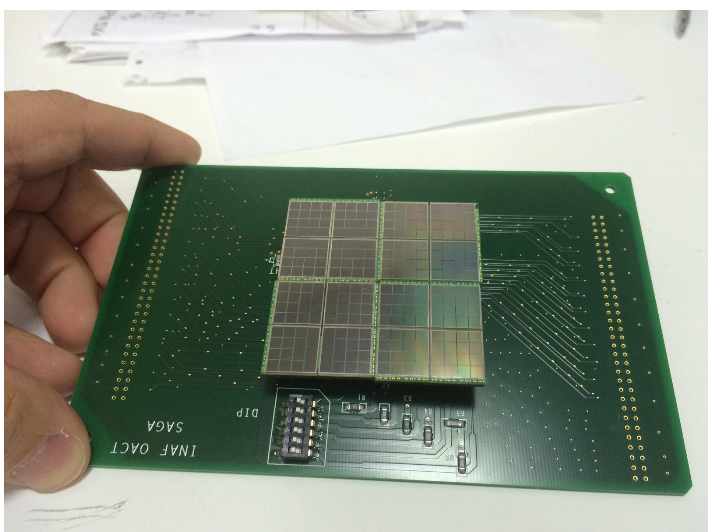

Figure 7. SiPM adapter board connected to the SiPM interface board.

An additional specific mechanical support, depicted in Figure 8, has been realized to house the MPPC detectors; in particular, a black light-tight box prevents accidental light exposure of the MPPC detectors and provides a thermal regulation by means of a home-made cooling system adopting a Peltier cell. A thermal calibration of the system allows to set and maintain the desired temperature.

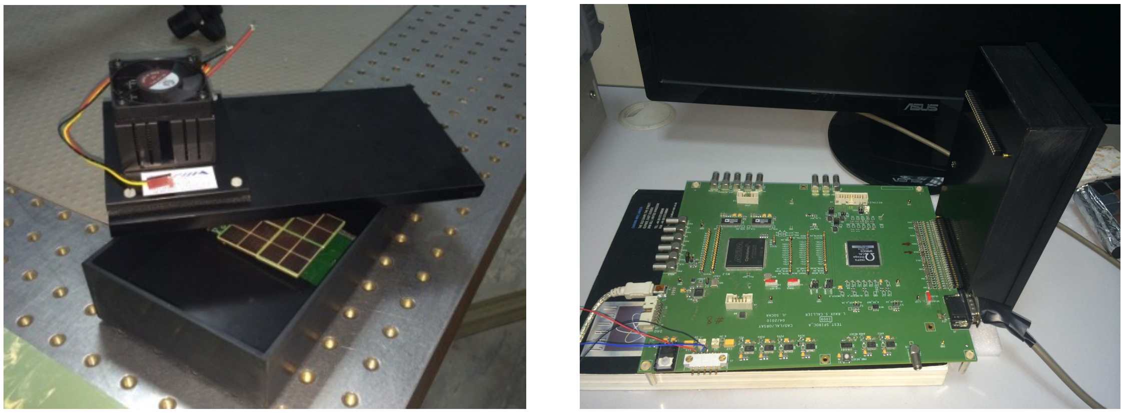

Figure 8. Mechanical support for SiPM housing and cooling system (on the left side) and mechanical system connected to the EASIROC evaluation board (on the right side).

4. SIPM CHARACTERIZATION RESULTS

This section presents and discusses the main characterization measurements on the basic 3×3mm^2 single-pixel of the S11828-3344 MPPC detector for the ASTRI SST-2M camera, carried out on the test facilities available at the COLD laboratory. In addition, a few measurement results on recently developed detectors are also shown, demonstrating outstanding performance for the ASTRI/CTA mini-array project.

4.1 Measurements on the ASTRI SST-2M Detectors

The detector gain determination, at a given temperature and for a defined range of bias voltages, is accomplished through a pulsed diode laser illuminating the SiPM housed in the CAEN PSAU. The integrated charge values from a multi-channel analyzer reading the PSAU output are filled into charge amplitude histograms and the average spacing between two adjacent curve peaks is computed (ADC channels). Consequently, by accounting for the constant ADC rate (charge/channel), and scaling by the amplifier gain factor, the sensor gain is obtained for a given bias voltage. Figure 9 illustrates the gain measurement results for the MPPC detector as a function of the bias voltage at T=25°C. The data fit demonstrates the linear behavior of the SiPM gain versus the operating voltage, and also allows extrapolation of the breakdown voltage at the x-axis intercept (70.5V).

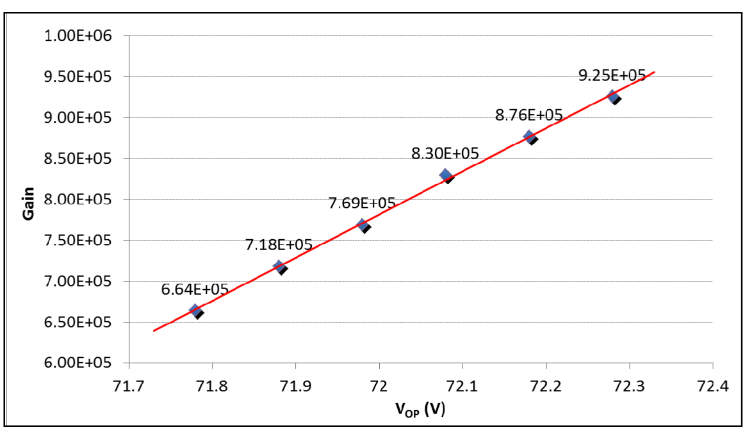

Figure 9. Gain measurements of the MPPC device as a function of the bias voltage at T=25°C. The linear fit allows to extrapolate the breakdown potential.

Dark current and optical cross-talk are the main crucial parameters affecting the performance of SiPM detectors. The Dark Count Rate (DCR) is defined as the number of avalanche current pulses produced by thermally generated carriers simulating the detection of single photons at a certain bias voltage. Since the dark noise is comprised of a series of time pulses, its magnitude is often quoted as a pulse rate, typically expressed in kHz or MHz.

Optical cross-talk occurs when optical photons that are emitted by accelerated charge carriers undergoing an avalanche propagate towards neighboring diode pixels where, depending on their energy and location, they have a certain probability to generate an additional Geiger avalanche discharge; as a consequence, since the original and neighbor avalanches may occur almost simultaneously (on the same scale of few nanoseconds), single absorbed photons may generate output signals equivalent to more than 1-pe (photoelectron) avalanche events. The experimental approach used for assessing the SiPM cross-talk probability relies on the analysis of DCR measurement results. By comparing the measured event rates above 1-pe threshold with the total dark rate the cross-talk probability is estimated.

Cross-talk and DCR measurements have been performed on the CAEN PSAU test bench. Experimental results of the MPPC detector for different operating voltages are illustrated in Figure 10 at T=25°C, where the rising trends of both parameters are observed.

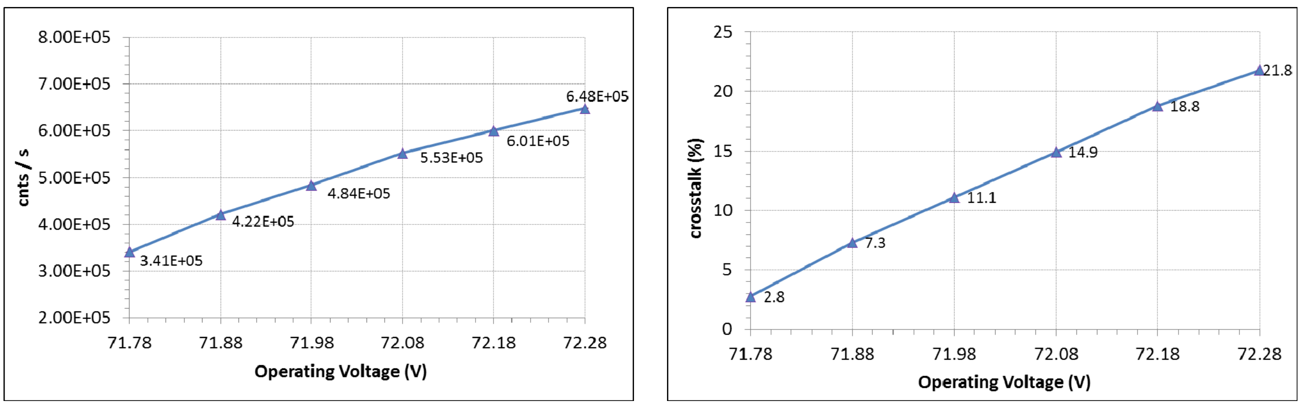

Figure 10. DCR (on the left) and optical cross-talk (on the right) measurement results of the MPPC device at T=25°C as a function of the operating voltage.

As inspected from the above plots, in the analyzed range of operating voltages the SiPM DCR and cross-talk values keep lower than 700kHz and 22%, respectively.

SiPM absolute Photon Detection Efficiency (PDE) measurements are performed based on the photon counting method, by which the number of pulses per unit time in monochromatic light conditions are compared to the light signal level recorded by a reference NIST photodetector at the same time and for several wavelengths [7].

Figure 11 illustrates the PDE measurements of the MPPC detector in the 350–950-nm range of wavelengths and for different operating conditions. A 320-ns hold-off time is applied for all curves to reduce as much as possible any extra-charge effects. Dark noise contributions are removed, as described in [16]-[17].

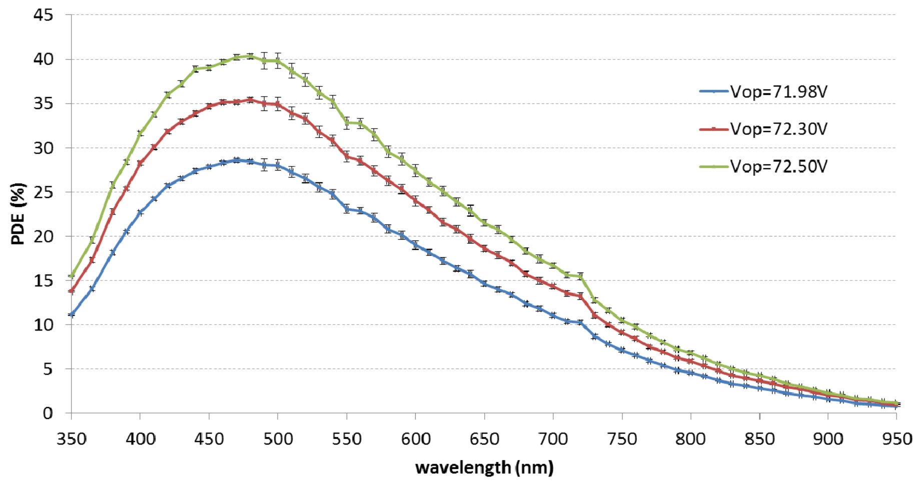

Figure 11. PDE measurements as a function of wavelength of the MPPC detector for different operating voltages and T=25°C.

As can be noted, for higher operating voltages PDE values increase, due to the higher trigger probability intrinsic to the device.

4.2 Measurements on other SiPM Detectors

In the framework of the ASTRI/CTA mini-array, succeeding phase of the ASTRI project, remarkable research studies and technological development in this class of detectors have been extensively undertaken by a rising number of companies and institutions. SiPM detectors promise to fulfill a wide set of requirements coming from a large number of emerging contexts, and several silicon foundries primarily driven by the physical and medical fields are currently investing in future development and innovation. Recently, new SiPM detectors with enhanced overall features have been produced by the world leading manufacturers, and further performance improvements are shortly foreseen.

In the following, measurement results are presented on some recently produced SiPM prototypes by two manufacturers, which have been sent to our laboratories for testing and evaluation purposes (and so are not commercially available at the moment), whose main basic features are summarized in Table 1.

Table 1. Main features of the tested SiPM detectors.

	Hamamatsu SN-1	**Excelitas D3932**	**Excelitas E3183**
Active area	3.0×3.0 mm^2	3.0×3.0 mm^2	6.0×6.0 mm^2
Microcells	3600	3600	14400
Pixel pitch	50 μm	50 μm	50 μm
Fill factor	61.5%	51.0%	40.0%

A DCR scan plot of the analyzed detectors in Table 1 for different values of the discriminator threshold, V_{TH}, is reported in Figure 12. The optimal threshold level of the discriminator used for PDE measurements for each device, also reported in Figure 12, can be determined by the DCR measures at half-photon threshold.

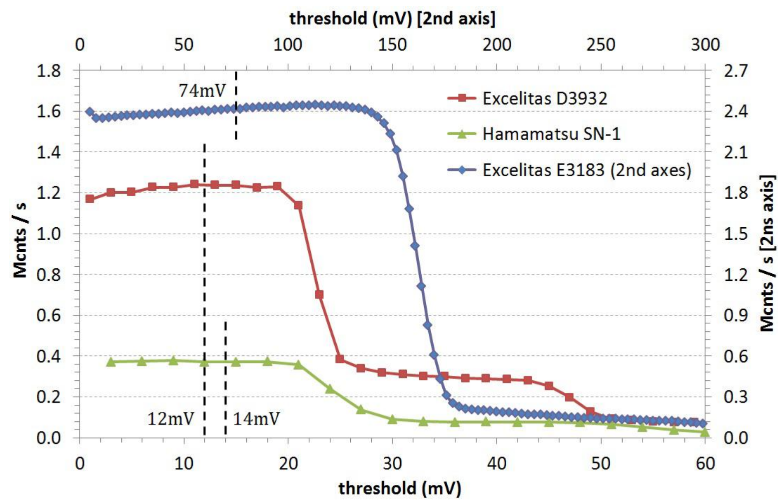

Figure 12. Dark staircase functions for the three analyzed detectors and relevant 0.5-pe thresholds determination.

Cross-talk and DCR measurement results of the three analyzed detectors at different operating voltages are illustrated in Figure 13, where the rising trends of both parameters are observed.

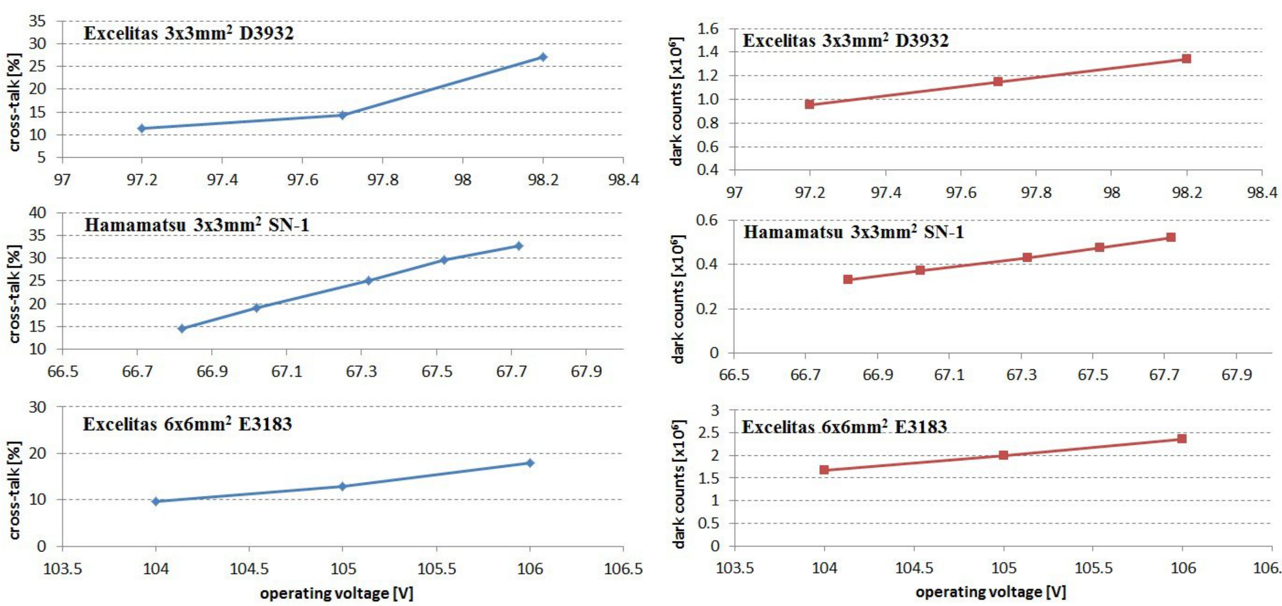

Figure 13. Cross-talk (on the left side) and DCR (on the right side) measurements results of the three analyzed SiPM detectors at different operating voltages.

To achieve a global comparison among the different SiPM detectors in terms of their most significant performance parameters, and to help choose the optimal operating condition for a specific device, Figure 14 and Figure 15 depict the PDE measurements of the three analyzed SiPMs at λ=450nm and T=25°C as a function of cross-talk and dark counts, respectively. Each single data curve in both plots implicitly reflects the cross-talk and DCR functional dependency on the bias conditions, as higher x-axis points for the same detector refer to increased operating voltages.

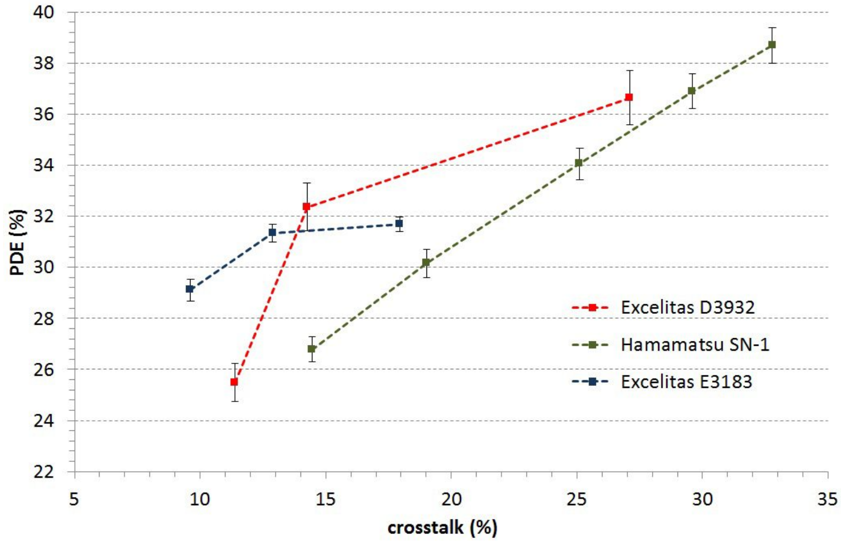

Figure 14. PDE versus cross-talk measurements of the analyzed SiPM detectors at λ=450nm and T =25°C.

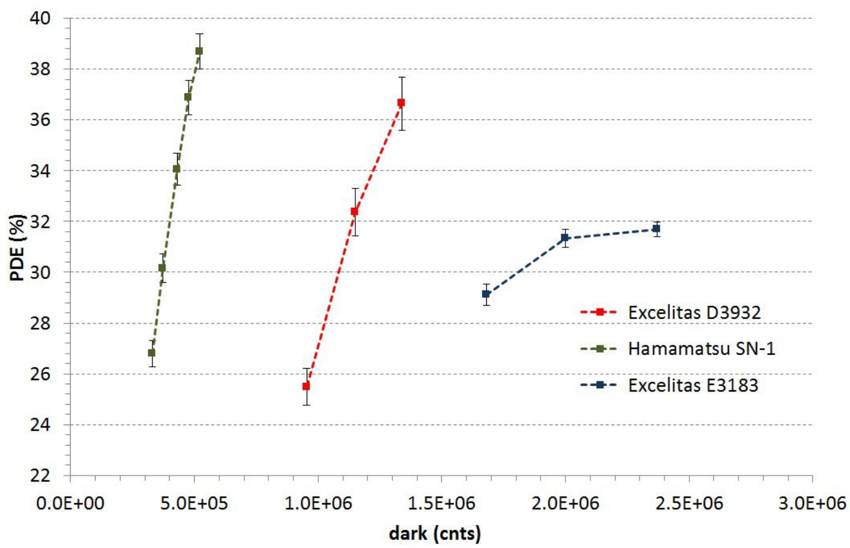

Figure 15. PDE versus DCR measurements of the analyzed SiPM detectors at λ=450nm and T =25°C. The Excelitas E3183 detector shows higher DCR values due to the larger device area.

These graphs are believed to be particularly significant and helpful in evaluating the best operating conditions for a particular SiPM detector as a result of an optimal trade-off between PDE and cross-talk, from one side, and PDE and DCR, from the other side; in fact, higher PDE values are obtained at greater operating voltages, at the cost of increased cross-talk and DCR. Moreover, the above plots can be usefully exploited for comparing the photon detecting capabilities of the characterized SiPMs within the maximum allowed values of the most important noise sources (cross-talk and dark) dictated by the specific application requirements.

It should be here remarked that the three analyzed SiPMs are not actually comparable in terms of DCR, because the Excelitas E3183 detector shows higher dark rates compared to the other devices due to the 4-times greater dimensions

5. CONCLUSIONS AND OUTLOOK

Measurement results from a systematic characterization methodology for the MPPC detectors of the ASTRI SST-2M camera and other recently produced SiPMs is discussed, with the aim of providing accurate measurements of the most important electro-optical parameters and qualifying the overall device performance. Experimental results of a large set of measurements on the basic MPPC device are performed, in order to provide a reliable qualification of the detector performance and evaluate its compliance with the telescope focal plane requirements. Other recently produced devices are being analyzed at our laboratories, and their foremost electrical and optical features are presently under evaluation.

ACKNOWLEDGMENTS

This work was partially supported by the ASTRI "Flagship Project" financed by the Italian Ministry of Education, University, and Research (MIUR) and led by the Italian National Institute of Astrophysics (INAF). We gratefully acknowledge support from the agencies and organizations listed in http://www.cta-observatory.org/?q=node/22.

REFERENCES

[1] M. Actis, *et al.*, The CTA Consortium, "Design Concepts for the Cherenkov Telescope Array CTA: An Advanced Facility for Ground-Based High-Energy Gamma-Ray Astronomy", *Experimental Astronomy*, vol. 32, issue 3, pp. 193-316, 2011.

[2] M. C. Maccarone, *et al.*, "The Site of the ASTRI SST-2M Telescope Prototype", *Proc. 33rd ICRC*, ArXiv: 1307.5139 (2013).

[3] O. Catalano, *et al.*, "The camera of the ASTRI SST-2M prototype for the Cherenkov Telescope Array", *Proc. SPIE Astronomical Telescopes + Instrumentation 2014*, Paper#9147-12, these proceedings, 2014.

[4] R. Canestrari, *et al.*, on behalf of the ASTRI collaboration, *32nd International Cosmic Ray Conference*, vol. 9, pp. 115-118, 2011.

[5] S. Cova, M. Ghioni, A. Lacaita, C. Samori, and F. Zappa, "Avalanche Photodiodes and Quenching Circuits for Single-Photon Detection", *Applied Optics*, vol. 35, no. 12, pp. 1956-1976, 1996.

[6] F. Zappa, S. Tisa, A. Tosi, and S. Cova, "Principles and features of single-photon avalanche diode arrays", *Sensors and Actuators A*, vol. 140, pp. 103-112, 2007.

[7] G. Bonanno, *et al.* "Precision Measurements of Photon Detection Efficiency for SiPM Detectors", *Nuclear Instruments and Methods in Physics Research A*, vol. 610, no. 1, pp. 93-97, 2009.

[8] S. Billotta, *et al.*,"Characterization of Detectors for the Italian Astronomical Quantum Photometer Project", *Journal of Modern Optics*, vol. 52, nos. 2-3, pp. 273-283, 2009.

[9] M. Belluso, *et al.*, "Characterization of SPAD Arrays: first results", in *Scientific Detectors for Astronomy*, J. E. Beletic, J.W. Beletic, and P. Amico, Eds., vol. LXIV, no. 771, p. 1-4020-4329-5, Berlin: Springer Dordrecht, p. 469, 2006.

[10] D. Marano, *et al.*, "Silicon Photomultipliers Electrical Model Extensive Analytical Analysis", *IEEE Transactions on Nuclear Science*, vol. 61, no. 1, pp. 23-34, 2014.

[11] D. Marano, *et al.*, "Improved SPICE Electrical Model of Silicon Photomultipliers", *Nuclear Instruments and Methods in Physics Research A*, vol. 726, pp. 1-7, 2013.

[12] D. Marano, *et al.*, "Accurate Analytical Single-Photoelectron Response of Silicon Photomultipliers", *IEEE Sensors Journal*, in press, DOI:10.1109/JSEN.2014.2316363.

[13] P. Eckert, H.-C. Schultz-Coulon, W. Shen, R. Stamen, and A. Tadday, "Characterisation Studies of Silicon Photomultipliers", *Nuclear Instruments and Methods in Physics Research A*, vol. 620, no. 1, pp. 217-226, 2010.

[14] A. Vacheretc, *et al.*, "Characterization and Simulation of the Response of Multi-Pixel Photon Counters to Low Light Levels", *Nuclear Instruments and Methods in Physics Research A*, vol. 656, no. 1, pp. 69-83, 2011.

[15] C. Piemonte, *et al.*, "Characterization of the First Prototypes of Silicon Photomultiplier Fabricated at ITC-irst", *IEEE Transactions on Nuclear Science*, vol. 54, no. 1, pp. 236-244, 2007.

[16] P. Finocchiaro, *et al.*, "Characterization of a Novel 100-Channel Silicon Photomultiplier – Part I: Noise", *IEEE Transactions on Electron Devices*, vol. 55, no. 10, pp. 2757-2764, 2008.

[17] P. Finocchiaro, *et al.*, “Characterization of a Novel 100-Channel Silicon Photomultiplier – Part II: Charge and Time”, *IEEE Transactions on Electron Devices*, vol. 55, no. 10, pp. 2765-2773, 2008.
[18] G. Pareschi, *et al.*, “The ASTRI/CTA mini-array of Small Size Telescopes Dual-Mirror: a first seed for the Cherenkov Telescope Array”, *Proc. SPIE Astronomical Telescopes + Instrumentation 2014*, Paper#9145-22, these proceedings, 2014.
[19] V. De Caprio, *et al.*, “The ASTRI SST-2M Prototype: Camera Design”, in *Proc. SPIE*, 2013.
[20] J. Fleury, *et al.*, “Petiroc and Citiroc: front-end ASICs for SiPM read-out and ToF applications”, JINST 9 C01049, 2014.
[21] S. Callier, C. de La Taille, G. Martin-Chassarda, L. Raux, “EASIROC, An Easy & Versatile Readout Device for SiPM”, in *Proc. TIPP*, 2001.